Heliyon 10 (2024) e26989

Contents lists available at ScienceDirect

Heliyon

journal homepage: www.cell.com/heliyon

Research article

Activated hedgehog gene pattern correlates with dismal clinical outcome and tumor microenvironment heterogeneity in hepatocellular carcinoma

Limin Zhen [a,b,1], Yi Zhu [a,c,1], Zhen Wu [a,b,1], Jinyao Liao [b], Liaoyuan Deng [d], Qianqian Ma [b], Qili Wu [e], Gang Ning [f], Qiuxiong Lin [e], Liya Zhou [g,**], Yanjie Huang [a,***], Zewei Zhuo [a,d,*], Ren Chen [b,****], Dongnan Yu [c,*****]

[a] *Guangdong Cardiovascular Institute, Guangdong Provincial People's Hospital, Guangdong Academy of Medical Sciences, Guangzhou, 510080, Guangdong, China*
[b] *Department of Infectious Diseases, Guangdong Provincial People's Hospital, Guangdong Academy of Medical Sciences, Guangzhou, 510080, Guangdong, China*
[c] *Department of Anesthesiology, Guangdong Provincial People's Hospital, Guangdong Academy of Medical Sciences, Guangzhou, 510080, Guangdong, China*
[d] *School of Medicine, South China University of Technology, Guangzhou, Guangdong 510006, China*
[e] *Medical Research Institute, Guangdong Provincial People's Hospital (Guangdong Academy of Medical Sciences), Southern Medical University, Guangzhou, 510080, China*
[f] *Department of Gastroenterology and Hepatology, Guangzhou Digestive Diseases Center, Guangzhou First People's Hospital, South China University of Technology, Guangzhou, Guangdong Province, China*
[g] *Department of Radiation Oncology, Hainan General Hospital, Hainan Affiliated Hospital of Hainan Medical University, Haikou, Hainan Province, China*

ARTICLE INFO

Keywords:
Hedgehog
Hepatocellular carcinoma
Clinical outcome
Tumor immunity
Immunotherapy

ABSTRACT

Background: Activation of the Hedgehog signaling pathway is linked to the initiation and development of human hepatocellular carcinoma (HCC). However, its impact on clinical outcomes and the HCC microenvironment remains unclear.
Methods: We performed comprehensive analyses of Hedgehog pathway genes in a large cohort of HCC patients. Specifically, we utilized univariate Cox regression analysis to identify Hedgehog genes linked to overall survival, and the LASSO algorithm was used to construct a Hedgehog-related gene pattern. We subsequently examined the correlation between the Hedgehog pattern and the HCC microenvironment employing the CIBERSORT and ssGSEA algorithms. Furthermore, Tumor Immune Dysfunction and Exclusion (TIDE) algorithm and the anti-PD-L1 treatment

* Corresponding author. Guangdong Cardiovascular Institute, Guangdong Provincial People's Hospital, Guangdong Academy of Medical Sciences, Guangzhou, 510080, Guangdong, China
** Corresponding author.
*** Corresponding author.
**** Corresponding author.
***** Corresponding author.
E-mail addresses: zhouliya1988@126.com (L. Zhou), hyj0106@foxmail.com (Y. Huang), zhuozewei@gdph.org.cn (Z. Zhuo), crlmczx@163.com (R. Chen), youngeryu@gdph.org.cn (D. Yu).
[1] These authors have contributed equally to this work.

https://doi.org/10.1016/j.heliyon.2024.e26989
Received 7 May 2023; Received in revised form 2 February 2024; Accepted 22 February 2024
Available online 28 February 2024

dataset (IMvigor210) are used to evaluate the clinical response of the Hedgehog pattern in predicting immune checkpoint inhibitors.
Results: We found that the Hedgehog activation score (HHAS), a prognostic score based on 11 Hedgehog genes, was significantly associated with HCC patient survival. Patients exhibiting high HHAS experienced markedly reduced survival rates compared to those with low HHAS, and HHAS emerged as an independent prognostic factor for HCC. Functional enrichment analysis unveiled the association of the HHAS phenotype with functions related to the immune system, and further investigation demonstrated that HCC patients exhibiting low HHAS displayed elevated levels of anti-tumor immune activation in $CD8^+$ T cells, while high HHAS were linked to immune escape phenotypes and increased infiltration of immune suppressive cells. In addition, in the Immune Checkpoint Inhibitor (ICI) cohort of IMvigor210, patients with higher HHAS had worse ICI treatment outcomes and shortened survival time, indicating that the HHAS is a useful indicator for predicting patient response to immunotherapy.
Conclusions: In summary, our study offers valuable insights for advancing research on Hedgehog and its impact on tumor immunity, which provides an opportunity to optimize prognosis and immune therapy for HCC.

1. Introduction

Liver cancer, specifically hepatocellular carcinoma (HCC), represents a significant and often fatal malignancy affecting the digestive system. Globally, it ranks as the second most prevalent cause of cancer-related fatalities [1]. Despite the established effectiveness of surgical removal, liver transplantation, and local ablation for early-stage HCC [2], the occurrence of recurrence remains high, affecting up to 70% of patients within five years. Unfortunately, there is currently no accompanying therapy available to address this issue [3].

The progression of HCC involves an intricate process frequently linked with the presence of liver cirrhosis, where repeated inflammation and fibrinogenesis predispose the liver to dysplasia and HCC transformation [4]. Notable etiological factors involve chronic hepatitis B or C infections, resulting in cirrhosis and the malignant transformation of hepatocyte due to persistent inflammation and viral-induced injury [5]. Furthermore, chronic liver injury and inflammation in conditions such as nonalcoholic steatohepatitis and alcoholic steatohepatitis may also contribute to liver fibrosis, subsequently progressing to cirrhosis and, ultimately, HCC [6]. Mechanistically, the Wnt/β-catenin pathway [7], and notably, the Hedgehog pathway [8] are increasingly recognized for their involvement in the initiation and development of HCC. Consequently, a comprehensive understanding of the pathogenesis is crucial, as

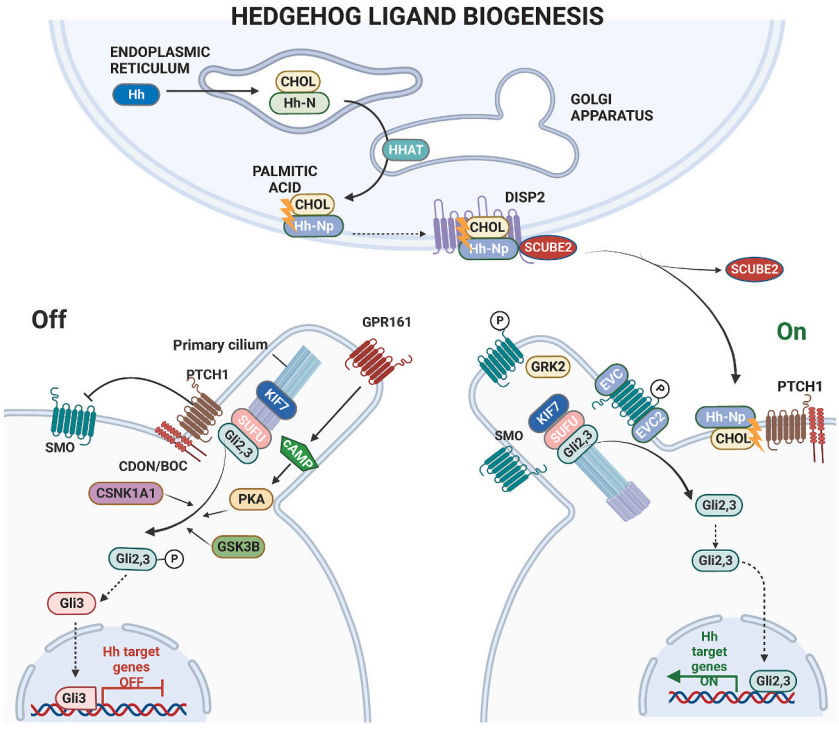

Fig. 1. Molecules and their interactions in Hedgehog signaling pathway.

it can help in the identification of reliable prognostic biomarkers that could potentially offer significant benefits to HCC patients during treatment.

A classic and conserved system, the Hedgehog signaling pathway plays a crucial role in maintaining embryonic development and the functionality of various adult tissues and organs. During tumorigenesis, abnormal Hedgehog activation contributes to the malignant transformation, progression, resistance, and metastasis of multiple solid tumors, including hepatocellular carcinoma [9–12]. Additionally, a research teams from The Cancer Genome Atlas Research Network have conducted extensive data analysis on genomic mutations, DNA methylation epigenetic changes, RNA expression, and protein expression in 363 cases of hepatocellular carcinoma from around the world [13]. They revealed intriguing associations, including the discovery of a significant role for the Sonic Hedgehog pathway (Shh pathway). Abnormal activation of this pathway was identified when p53 mutations, DNA methylation, and viral integration coincided. The Shh pathway was activated in approximately half of the HCC samples, providing new insights into its previously not fully understood role in liver cancer. Therefore, we selected the Hedgehog signaling pathway as the focal point of our research with the anticipation of uncovering its significant value in HCC prognosis.

As shown in Fig. 1, the Hedgehog (Hh) signaling pathway alternates between 'off' and an 'on' states to finely control an intracellular signaling cascade that directly affects the Gli transcription factors [14–17]. When the Hh ligand is not present, Gli proteins within the cytoplasm are cleaved, producing a truncated version that translocates to the cell nucleus to inhibit the transcription of target genes. Conversely, Hh binding to the Patched (PTC) receptor on the cell's surface stabilizes the Gli proteins, enabling them to maintain their full-length, transcriptionally active form. This, in turn, promotes the expression of genes that are dependent on Hedgehog signaling. Multiple researches demonstrated that the key signaling molecules, such as PTCH1, SMO, GLI1/2/3, are frequently overexpressed in malignant tissues, serving as significant biomarkers for progression and prognosis [11,18]. The Hedgehog pathway is linked to specific functions of both the innate and adaptive immune systems [19]. Nevertheless, its role in the immune

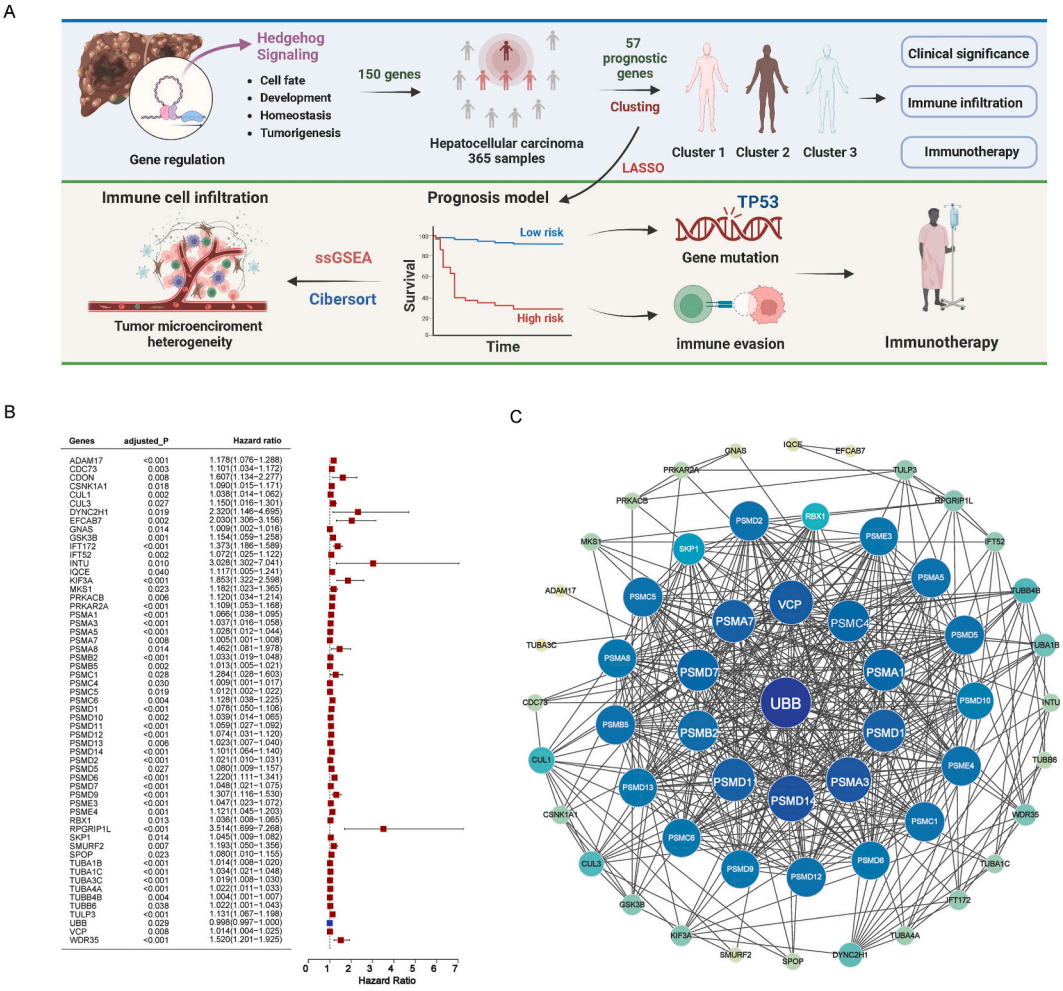

Fig. 2. Selection of Hedgehog genes associated with prognosis in HCC. (A) Flowchart of the analysis process in this study. (B) 57 Hedgehog genes significantly associated with survival ($P < 0.05$) were identified through univariate regression analysis. (C) The protein-protein interaction (PPI) network shows the correlation among the Hedgehog genes associated with prognosis.

response remains unclear and its association with liver cancer immunity and prognosis still requires further investigation.

Considering the pivotal role of the Hedgehog signaling pathway in tumor growth, we proposed a prognostic modeling in HCC based on the biological function of Hedgehog-related genes. The analytic workflow is summarized in Fig. 2A. The proposed prognostic model could provide a comprehensive analysis of the immune infiltration state and prognostic improvement in HCC patients, which makes it a promising diagnosis pattern for HCC and guide immunotherapy for clinical patients.

2. Materials and methods

2.1. Data Collection and processing for HCC patients

Obtained RNA-seq data (FPKM) and clinical information for 375 HCC patient tissues, along with 50 normal tissues from The Cancer Genome Atlas (TCGA)-LIHC cohort in the TCGA database (https://portal.gdc.cancer.gov/projects/TCGA-LIHC). For external validation, we collected RNA-seq data and related clinical details for 243 and 115 HCC patients from the International Cancer Genome Consortium (ICGC)-LIRI-JP and GSE76427 cohorts in the ICGC and (Gene Expression Omnibus) GEO databases, respectively. Table 1 presented the clinicopathologic characteristics HCC patients from these three cohorts. To reach the final gene expression values, we first removed data with gene expression values of 0, and used the average RNA expression value for multiple values. For the transcriptional profile in TCGA or ICGC, the downloaded normalized FPKM values or normalized read count were log2(data+1)-transformed for further analyses. To address batch effects in the GEO microarray data, we applied the "sva" package in R [20] for elimination. Subsequent data normalization was performed by the "limma" package in R [21], and the normalized data were also log2-transformed for further analyses. In addition, we downloaded a geneset of the Hedgehog signaling pathway from the Reactome Pathway Database (see Supplementary Table 1).

2.2. Identification hedgehog genes associated with prognosis

We utilized a univariate Cox regression analysis for the identification of prognostically relevant genes within the Hedgehog gene set. Subsequently, we performed protein-protein interaction (PPI) investigation to explore hub genes involved in HCC using the STRING database (version 12.0).

2.3. Consensus clustering analysis

To characterize HCC subgroups exhibiting comparable gene expression patterns, we performed consensus analysis using the ConsensusClusterPlus R package [22]. We used a maximum cluster number of 6, 100 repetitions, a subsample rate of 80%, clusterAlg = "hc", and innerLinkage = 'ward.D2'. We visualized the clustering results with the "pheatmap" package (https://CRAN.R-project.org/package=pheatmap). Statistical analysis of the clinical characteristics of HCC subgroups was conducted using R software, and the findings were depicted using the "ggplot2" package (https://CRAN.R-project.org/package=ggplot2).

2.4. Immune scoring

To evaluate immune level in various HCC subgroups, we utilized the xCell algorithm in the R package "immunedeconv" [23] for immune cell score analysis. The "immunedeconv" integrates six advanced deconvolution algorithms, including CIBERSORT, EPIC, xCell, TIMER, MCP-counter, and quanTIseq, each having undergone systematic benchmark testing. Among them, the xCell algorithm is categorized under marker gene-based approaches, relying on specific gene sets that indicate distinct cell types. This approach enables

Table 1
149 genes of the Hedgehog pathway.

Hedgehog pathway Gene									
ADAM17[a]	ADCY1	ADCY10	ADCY2	ADCY3	ADCY4	ADCY5	ADCY6	ADCY7	ADCY8
ADCY9	ARRB1	ARRB2	BOC	BTRC	**CDC73**[a]	**CDON**[a]	**CSNK1A1**[a]	**CUL1**[a]	**CUL3**[a]
DERL2	DHH	DISP2	**DYNC2H1**[a]	DZIP1	**EFCAB7**[a]	ERLEC1	EVC	EVC2	FUZ
GAS1	GAS8	GLI1	GLI2	GLI3	**GNAS**[a]	GPC5	GPR161	GRK2	**GSK3B**[a]
HHAT	HHIP	IFT122	IFT140	**IFT172**[a]	**IFT52**[a]	IFT57	IFT88	IHH	**INTU**[a]
IQCE[a]	ITCH	**KIF3A**[a]	KIF7	**MKS1**[a]	NOTUM	NUMB	OFD1	OS9	P4HB
PRKACA	**PRKACB**[a]	PRKACG	PRKAR1A	PRKAR1B	**PRKAR2A**[a]	PRKAR2B	**PSMA1**[a]	PSMA2	**PSMA3**[a]
PSMA4	**PSMA5**[a]	PSMA6	**PSMA7**[a]	**PSMA8**[a]	PSMB1	PSMB10	PSMB11	**PSMB2**[a]	PSMB3
PSMB4	**PSMB5**[a]	PSMB6	PSMB7	PSMB8	PSMB9	**PSMC1**[a]	PSMC2	PSMC3	**PSMC4**[a]
PSMC5[a]	**PSMC6**[a]	**PSMD1**[a]	**PSMD10**[a]	**PSMD11**[a]	**PSMD12**[a]	**PSMD13**[a]	**PSMD14**[a]	**PSMD2**[a]	PSMD3
PSMD4	**PSMD5**[a]	**PSMD6**[a]	**PSMD7**[a]	PSMD8	**PSMD9**[a]	PSME1	PSME2	**PSME3**[a]	**PSME4**[a]
PSMF1	PTCH1	**RBX1**[a]	**RPGRIP1L**[a]	RPS27A	SCUBE2	SEL1L	SEM1	SHH	**SKP1**[a]
SMO	SMURF1	**SMURF2**[a]	**SPOP**[a]	SPOPL	SUFU	SYVN1	TTC21B	TUBA1A	**TUBA1B**[a]
TUBA1C[a]	**TUBA3C**[a]	TUBA3D	**TUBA4A**[a]	TUBB1	TUBB2A	TUBB2B	TUBB3	TUBB4A	**TUBB4B**[a]
TUBB6[a]	**TULP3**[a]	UBA52	**UBB**[a]	UBC	ULK3	**VCP**[a]	WDR19	**WDR35**[a]	

[a] the genes associated to overall survival.

the independent quantification of each immune cell type by analyzing marker gene expression levels in complex samples. We used the "pheatmap" of R package to generate an expression heatmap. We extracted immune checkpoint-related gene expression values from HCC transcriptome data and utilized the "ggplot2" package to display the expression status of these genes. The Tumor Immune Dysfunction and Exclusion (TIDE) analysis were employed to forecast potential responses to immune treatment.

2.5. Developing and validating a hedgehog scoring model in HCC patients

Employing the least absolute shrinkage and selection operator (LASSO) algorithm, we narrowed down the scope of differential genes. Using the LASSO Cox regression model coefficients, we constructed a Hedgehog scoring model for HCC patients. The Hedgehog score calculation formula is as follows: Hedgehog score= (Coefficient of mRNA1 * mRNA1 expression level)+ (Coefficient of mRNA2*mRNA2 expression level)……+ (Coefficient of mRNAn*mRNAn expression level). Using the median Hedgehog score as the criterion, we categorized HCC patients into groups characterized as high-risk and low-risk patients. We generated Kaplan-Meier survival curves for the Hedgehog scores to evaluate survival differences between groups utilizing the "survival" package in R (https://CRAN.R-project.org/package=survival). We utilized the "timeROC" package in R [24] to produce receiver operating characteristic (ROC) curves, assessing the predictive accuracy of the Hedgehog scoring model. Prognostic significance in HCC patients was examined through the application of univariate and multivariate Cox regression analyses, considering clinical factors such as age, sex, race, and TNM stage, along with the Hedgehog score. We used the "forestplot" of R package (https://CRAN.R-project.org/package=forestplot) to plot the P-values and 95% confidence intervals of each variable. External cohorts (ICGC-LIRI-JP and GSE76427) were used to validate the stable of Hedgehog scoring model.

2.6. Mutation analysis

HCC mutation data was obtained from the TCGA online database, and mutation information was extracted. Patients with HCC were grouped based on their Hedgehog score, and a waterfall plot was generated using the "maftools" package [25] in R to visualize the mutation landscape for each Hedgehog score group.

2.7. Correlation analysis of hedgehog score with TME

Differential gene expression analysis between high-risk and low-risk groups in the TCGA cohort was conducted through the "limma" package in R. The cutoff value was set to $\log2|\text{fold change}| > 1$, and the false discovery rate (FDR) was <0.05. Functional enrichment analysis involved utilizing GO analysis on the differentially expressed genes (DEGs). The Immune, Stromal, and Estimate scores were determined through The ESTIMATE algorithm, which estimates stromal and immune cells in malignant tumor tissues using expression data. Using CIBERSORT, the relationship between the high-risk and low-risk groups was explored based on the candidate gene features and the abundance of each immune cell type. The "gsva" R package [26] was utilized for single-sample gene set enrichment analysis (ssGSEA).

Table 2
Clinicopathologic characteristics HCC patients.

	TCGA-LIHC	ICGC-LIRI-JP	GSE76427
No. of patients	365	243	115
Age (%)			
<45	42(11.5%)	5(2.1%)	7(6.08%)
≥45	323(88.5%)	238(97.9%)	108(93.92%)
Gender (%)			
Female	119(32.6%)	61(25.1%)	22(19.13%)
Male	246(67.4%)	182(74.9%)	93(80.87%)
Grade (%)			
Grade 1	55(15.1%)	NR	NR
Grade 2	175(47.9%)	NR	NR
Grade 3	118(32.3%)	NR	NR
Grade 4	12(3.3%)	NR	NR
unknown	5(1.4%)	NR	NR
Tumor Stage (%)			
I	170(46.6%)	36(14.8%)	55(47.83%)
II	84(23.0%)	110(45.3%)	35(30.43%)
III	83(22.7%)	76(31.3%)	21(18.26%)
IV	4(1.09%)	21(8.6%)	3(2.61%)
unknown	24(6.6%)		1(0.87%)
Survival status			
OS days (median)	556	780	423.4
Censored (%)	126(34.5%)	44 (18.1%)	23(20%)

NR: not reported.

2.8. Immune therapy prediction analysis

The tumor immune dysfunction and exclusion (TIDE) score served as the metric to evaluate the predictive capability for potential immune therapy responses in hepatocellular carcinoma (HCC). We leveraged the clinical cohort IMvigor210 to evaluate the predictive efficacy of distinct Hedgehog score groups in immune therapy. Through the Kaplan-Meier method, we conducted a comparative analysis of survival differences between the two Hedgehog score groups within the immune therapy cohort.

2.9. Statistical analysis

All the aforementioned analytical procedures were executed in R version 4.2.2. Distribution of clinical features was evaluated using the chi-square test, yielding corresponding p-values. Kaplan-Meier curves were subjected to log-rank test for obtaining p-values. Significance between two sample groups was assessed using the Wilcoxon test, while the Kruskal-Wallis test was employed for evaluating significance between three sample groups. Unless explicitly stated otherwise, significance was attributed to a p-value less than 0.05.

3. Results

3.1. Hedgehog signaling-related genes profiling identified three HCC clusters

A total of 149 genes related to Hedgehog signaling pathway were obtained from Reactome Pathway Database (Table 2). Through univariate Cox regression analysis, 57 survival-associated genes were identified. (Fig. 2B). Further analysis of protein-protein interactions revealed that UBB, PSMD14, and PSMA3 had the strongest gene interaction relationships, indicating that these genes may be critical targets for HCC prognosis (Fig. 2C). Utilizing the 57 prognosis-related genes associated with the Hedgehog signaling pathway, consensus clustering analysis was performed on HCC patients within the TCGA dataset. The results showed that when K = 2 or 3, the

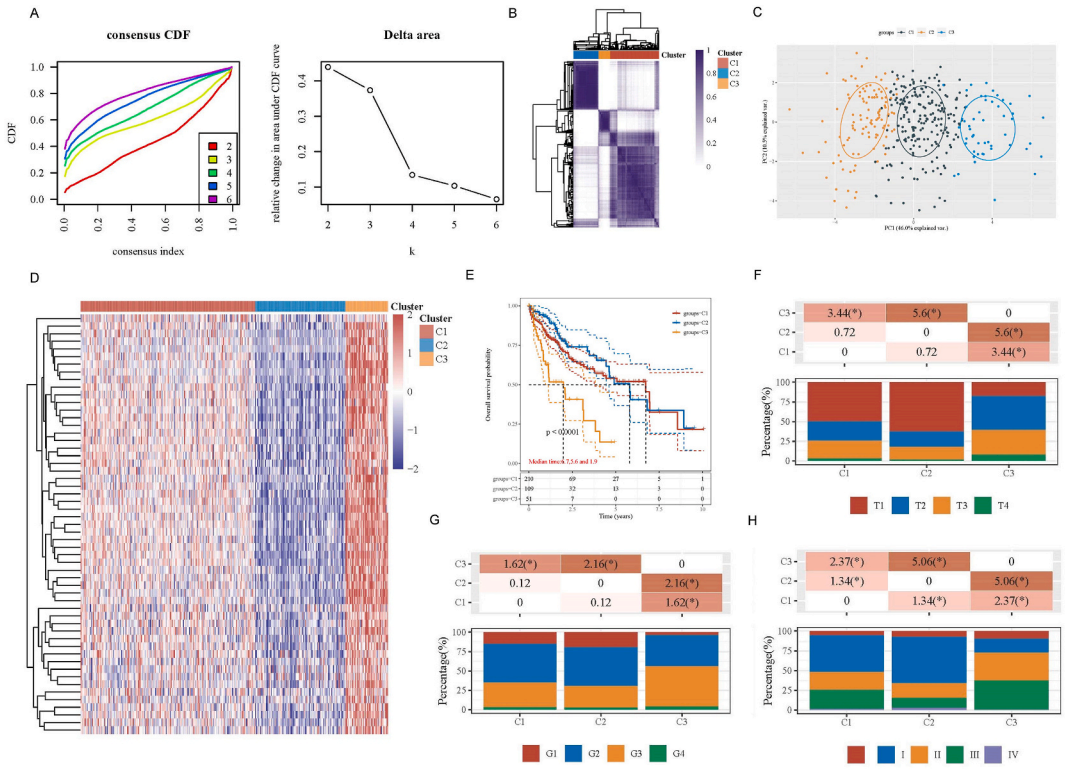

Fig. 3. Molecular subtyping based on prognostic Hedgehog genes. (A) Consensus clustering cumulative distribution function (CDF) and relative change in the area under the CDF curve (CDF Delta area) are shown. (B) Heat map of consensus clustering results with k = 3. (C) Principal component analysis (PCA) plot of the three subgroups. (D) Heat map of Hedgehog gene expression in different subgroups, with red indicating high expression and blue indicating low expression. (E) Kaplan-Meier survival curves for different subgroups, with log-rank test for inter-group comparison, and median time indicating the time corresponding to 50% survival (i.e., median survival time) in different groups, with the unit in years. (F) Distribution of T stage in different subgroups. (G) Distribution of Grade staging in different subgroups. (H) Distribution of Stage staging in different subgroups. The p-values of the chi-square test for the significance analysis are presented, with the numeric value representing the -log10(p–value). * indicates a significant difference in the distribution of the clinical features between the two corresponding groups ($p < 0.05$).

Consensus Cumulative Distribution Function (CDF) Delta area was the largest (Fig. 3A). When K = 3, the boundaries between the clusters were more distinct (Fig. 3B). Principal Component Analysis (PCA) confirmed the effective classification of HCC patients into three subgroups. Cluster 1 comprised 210 samples, Cluster 2 had 109 samples, and Cluster 3 included 51 samples (Fig. 3C). Fig. 3D shows the heatmap of Hedgehog signaling-related gene expression in the three subgroups, with most genes showing high expression in Cluster 3. Furthermore, an examination of the clinical significance of Hedgehog-related subgroups revealed that patients in Cluster 3 exhibited a markedly lower survival rate compared to those in Cluster 1 and Cluster 2 ($P < 0.00001$, Fig. 3E). Furthermore, we examined the correlation between the three subgroups and clinical features (Fig. 3F–H). The findings indicated a significantly higher proportion of T3+T4 stage, G3+G4 grade, and Stage II + III samples in Cluster 3 compared to Cluster 1 and Cluster 2. Conversely, the proportion of T1 stage, G1 grade, and Stage I samples was notably lower in Cluster 3 than in Cluster 1 and Cluster 2. These results suggest that the Hedgehog gene activation subtypes associates with the worse HCC prognosis and advanced HCC. Additionally, we further analyze the association between activation angiogenic factors (angiopoietin-1 (ANG1) and angiopoietin-2 (ANG2)), cyclins (cyclin D1(CCND1) and cyclin B1 (CCNB1)), anti-apoptotic genes (FAS) with Hedgehog pathway. Our results, as depicted in Supplementary Fig. 1, reveal that, relative to Hedgehog inactivation patients, those with Hedgehog pathway activation exhibit significant

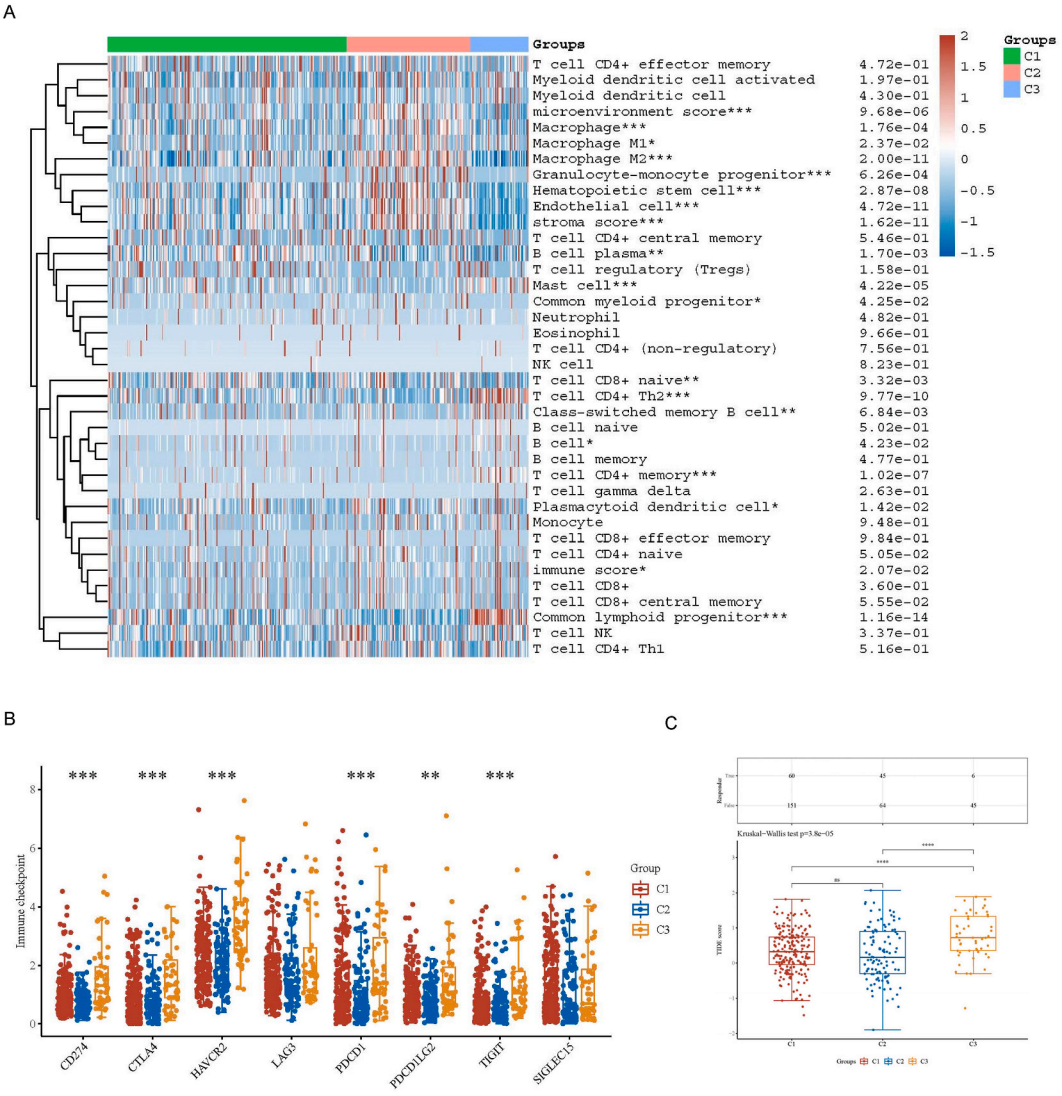

Fig. 4. Immune infiltration levels and immune therapy response analysis among three Hedgehog subgroups. (A) Heatmap of immune cell scores analyzed by the Xcell algorithm. (B) Heatmap of immune checkpoint-related gene expression. (C) Prediction of immune checkpoint inhibitor response based on the Tumor Immune Dysfunction and Exclusion (TIDE) algorithm for Hedgehog molecular subtypes. The upper table displays the number of samples with predicted immune responses in different groups, and the lower plot shows the distribution of predicted immune response scores in different groups. Different colors represent expression trends in different samples. *$p < 0.05$, **$p < 0.01$, ***$p < 0.001$, where the asterisks indicate the level of significance (*p). Significance among the three sample groups was determined by the Kruskal-Wallis test. (For interpretation of the references to color in this figure legend, the reader is referred to the Web version of this article.)

increases in Ang-1, Ang-2, CCND1, CCNB1, and FAS expression levels. This suggests that Hedgehog pathway activation may enhance angiogenesis, cell cycle progression, and reduce apoptosis, thus promoting disease progression in liver cancer.

3.2. Hedgehog-signaling related molecule subtypes correlates to the immune microenvironment

Xcell algorithm were applied to assess variations in the tumor microenvironment (TME) across distinct Hedgehog clusters. Our findings demonstrated that Cluster 3 exhibited significantly increased expression of immune-suppressive cells, including T cell $CD4^+$ Th2, T cell $CD4^+$ memory, and mast cells, while Cluster 2 showed significantly elevated expression of endothelial cells, hematopoietic stem cells, and granulocyte-monocyte progenitors (Fig. 4A). The vital function of immune checkpoint molecules lies in suppressing immune responses and fostering tumor immune escape within the immune system [27]. In our exploration of immune checkpoint gene expression across the three subgroups, Cluster 3 exhibited significant elevations in CD274, CTLA4, HAVCR2, PDCD1, PDCD1LG2, and TIGIT (Fig. 4B), suggesting a higher level of immune suppression. Furthermore, the response of the three subtypes to immune checkpoint inhibitors was predicted using the Tumor Immune Dysfunction and Exclusion (TIDE) algorithm [28]. Significantly higher TIDE scores were observed in Cluster 3 compared to the other clusters. The response rate to immune checkpoint inhibitors in Cluster 3 was notably lower at 11.76%, a statistically significant difference from the other two groups (Cluster 1: 28.43%, Cluster 2: 41.28%). (Fig. 4C). These findings imply that immune-suppressive cells and immune checkpoint genes within the tumor microenvironment could contribute to the unfavorable prognosis observed in Cluster 3.

3.3. Development a Distinctive hedgehog gene Signature for HCC

In the pursuit of a multi-gene prognostic score model, we implemented the LASSO regression algorithm to refine the selection of Hedgehog genes. A total of 11 Hedgehog genes were ultimately included in the prognostic model construction, with a minimum lambda value of 0.0442. The calculation formula for the Hedgehog activation score (HHAS) was as follows:

HHAS=(0.0035)*CUL1+(0.1641)*IFT172+(0.0141)*PRKAR2A+(0.112)*PSMA3+(0.0271)*PSMA7+(0.1285)*PSMB2+(0.0847)*PSMB5+(0.3073)*PSMD1+(0.0121)*PSMD13+(0.0966)*PSMD14+(−0.2054)*UBB.

According to the median HHAS (Fig. 5A), HCC patients from the TCGA dataset were divided into high-HHAS group (n = 182) and low-HHAS group (n = 183). As the HHAS increased, the number of deaths in HCC patients also significantly increased, and the survival time was significantly shortened (Fig. 5B). The PCA plot showed good differentiation between two HHAS populations (Fig. 5C). The Kaplan-Meier curve unveiled a markedly decreased overall survival rate for patients in the low-HHAS group as opposed to those in the high-HHAS group (Fig. 5D, P = 9.4215e-08). Assessing the prognostic performance of the HHAS using the time-varying ROC curve revealed that, at 1 year, the area under the curve (AUC) was 0.723, at 3 years it stood at 0.706, and at 5 years, it reached 0.721 (Fig. 5E), indicating that the HHAS had a high prognostic predictive ability. Conducting univariate and multivariate regression analyses underscored the autonomy of Stage and HHAS as pivotal prognostic factors in HCC patient outcomes. The independent significance of both Stage and HHAS in predicting patient prognosis was established through these analyses (Fig. 5F). By analyzing the

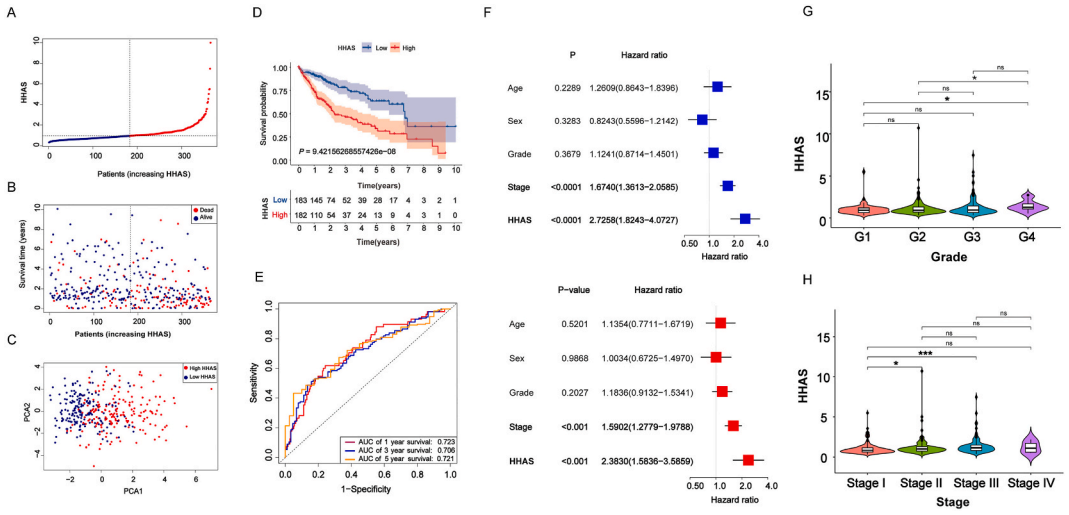

Fig. 5. Development of a prognostic model based on the Hedgehog genes associated with patient outcomes. (A) HCC patients were stratified into high-HHAS and low-HHAS groups based on the median risk score. (B) Distribution of the survival status of HCC patients based on HHAS. (C) Principal component analysis plot for different HHAS groups. (D) Kaplan-Meier (KM) survival curves for the HHAS model in the TCGA dataset, with different groups compared by log-rank test. (E) Time-dependent ROC curves and AUC values for the HHAS model at different time points, with a higher AUC indicating a stronger predictive ability of the model. (F) Univariate and multivariate Cox regression analysis of clinical features to identify independent prognostic factors for HCC patients. (G) Distribution of Grade staging between high-HHAS and low-HHAS groups. (H) Distribution of Stage staging between high-HHAS and low-HHAS groups.

relationship between the HHAS distribution and different pathological stages of HCC patients, we found that the HHAS of G4 stage was significantly different from that of G1 and G2 stages (Fig. 5G), and the HHAS of Stage III was significantly different from that of Stage I (Fig. 5H), indicating that HHAS was closely related to tumor prognosis and progression.

3.4. The HHAS model exhibits robust prognostic prediction ability

The HHAS model was further validated using two independent external datasets. Similarly, according to the median HHAS, HCC patients in the ICGC-LIRI-JP and GSE76427 cohorts were precisely categorized into high- and low-HHAS groups (Fig. 6A and F). With an elevation in HHAS levels, there was a notable reduction in the survival time of HCC patients within both cohorts. The increase in HHAS demonstrated a significant correlation with a decrease in the survival duration among patients in both study groups (Fig. 6B and G). PCA plots also demonstrated the precise stratifying power of the HHAS model (Fig. 6C and H). Illustrated in Fig. 6D and I, the overall survival rate exhibited a substantial decline among high-HHAS patients when compared to their low-HHAS counterparts (ICGC-LIRI-JP cohorts, P = 0.0001406; GSE76427, 9.88e-06). Survival prediction metrics for the ICGC-LIRI-JP cohort demonstrated AUCs of 0.697, 0.713, and 0.701 at 1, 2, and 3 years, respectively (Fig. 6E). Similarly, in the GSE76427 cohort (Fig. 6J), the AUCs stood at 0.787, 0.7762, and 0.78 for the same respective time points. These findings affirm the robust survival prediction capabilities of the HHAS model, suggesting its applicability in forecasting HCC prognosis.

3.5. High HHAS patients have increased TP53 mutation rates

Delving deeper into our investigation, we scrutinized somatic mutations among HCC patients with varying HHAS levels. Highlighted in the results is a greater proportion of patients with mutations in the high-HHAS group as opposed to the low-HHAS group (79.21% vs. 73.6%) (Fig. 7A–B). The high-HHAS group exhibited a significantly higher proportion of TP53 mutations compared to the low-risk group (37% vs. 22%). Conversely, the low-risk patients exhibited a notably higher prevalence of CTNNB1 mutations compared to the high-risk group (30% vs. 21%). In addition, patients with TP53 mutations in the high-HHAS group had multiple mutation types, including frameshift insertions, nonsense mutations, frameshift deletions, and missense mutations. Implying a potential association, these findings indicate that the elevated incidence of TP53 mutations might contribute to the adverse prognosis observed in the high-HHAS group.

3.6. Immunosuppressive-related cells Selectively activate in high HHAS patients

In the cluster model, we performed GO functional enrichment analysis, revealing that DEGs among HHAS subgroups were predominantly enriched in immune-related biological processes, immunological synapse formation, like establishment of T cell polarity, and dendritic cell apoptotic process (Fig. 8A). These results suggest that the HHAS may be influenced by immunogencity. Implementing the ESTIMATE algorithm, we evaluated immune-related scores in HCC patients sourced from the TCGA database. Our investigation unveiled a noteworthy decline in the immune score, stromal score, and estimate score within the high-HHAS group compared to the low-HHAS group (Fig. 8B). This signifies that the high-HHAS group demonstrated a comparatively lower abundance of immune cells and stromal cells. Subsequent to this, an evaluation of the correlation between the HHAS model and TME features was

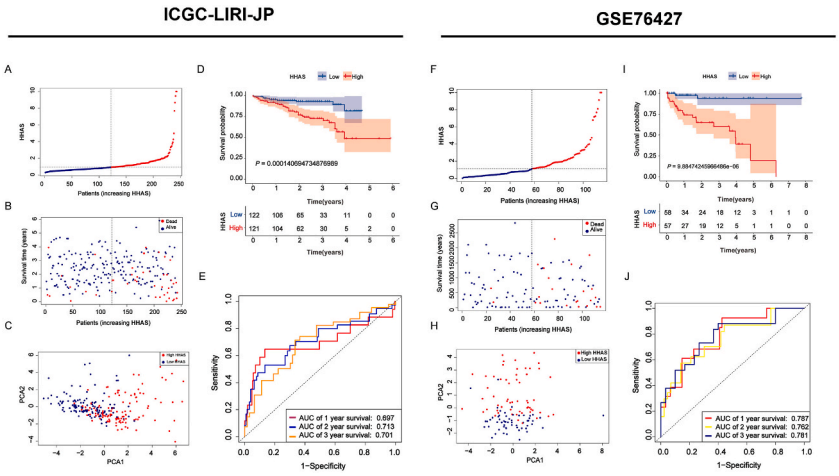

Fig. 6. Robustness of the HHAS model validated by external data sets. (A, F) The HCC patients from ICGC-LIRI-JP and GSE76427 cohorts were stratified into high- and low-HHAS groups based on the median HHAS score. (B, G) Survival status distribution of HCC patients in ICGC-LIRI-JP and GSE76427 cohorts based on the HHAS. (C, H) Principal component analysis (PCA) plots of HCC patients in different HHAS groups from ICGC-LIRI-JP and GSE76427 cohorts. (D, I) Kaplan-Meier survival curves of the HHAS model in ICGC-LIRI-JP and GSE76427 cohorts. (E, J) ROC curves of the HHAS model at different time points in ICGC-LIRI-JP and GSE76427 cohorts.

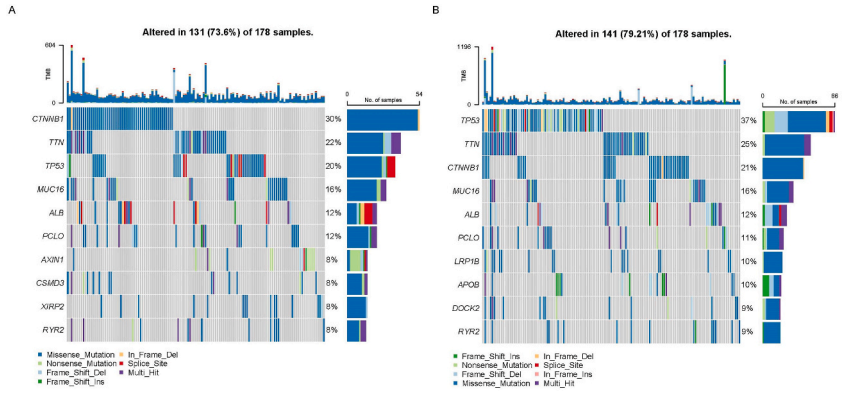

Fig. 7. Prediction of gene mutations by the HHAS model. (A) Waterfall plot of gene mutations in the low-HHAS group. Mutations were detected in 73.6% of HCC patients, with CTNNB1 being the main mutated gene (30%). (B) Gene mutation status in the high-HHAS group. Gene mutations were detected in 79.21% of HCC patients, with TP53 being the main mutated gene (37%).

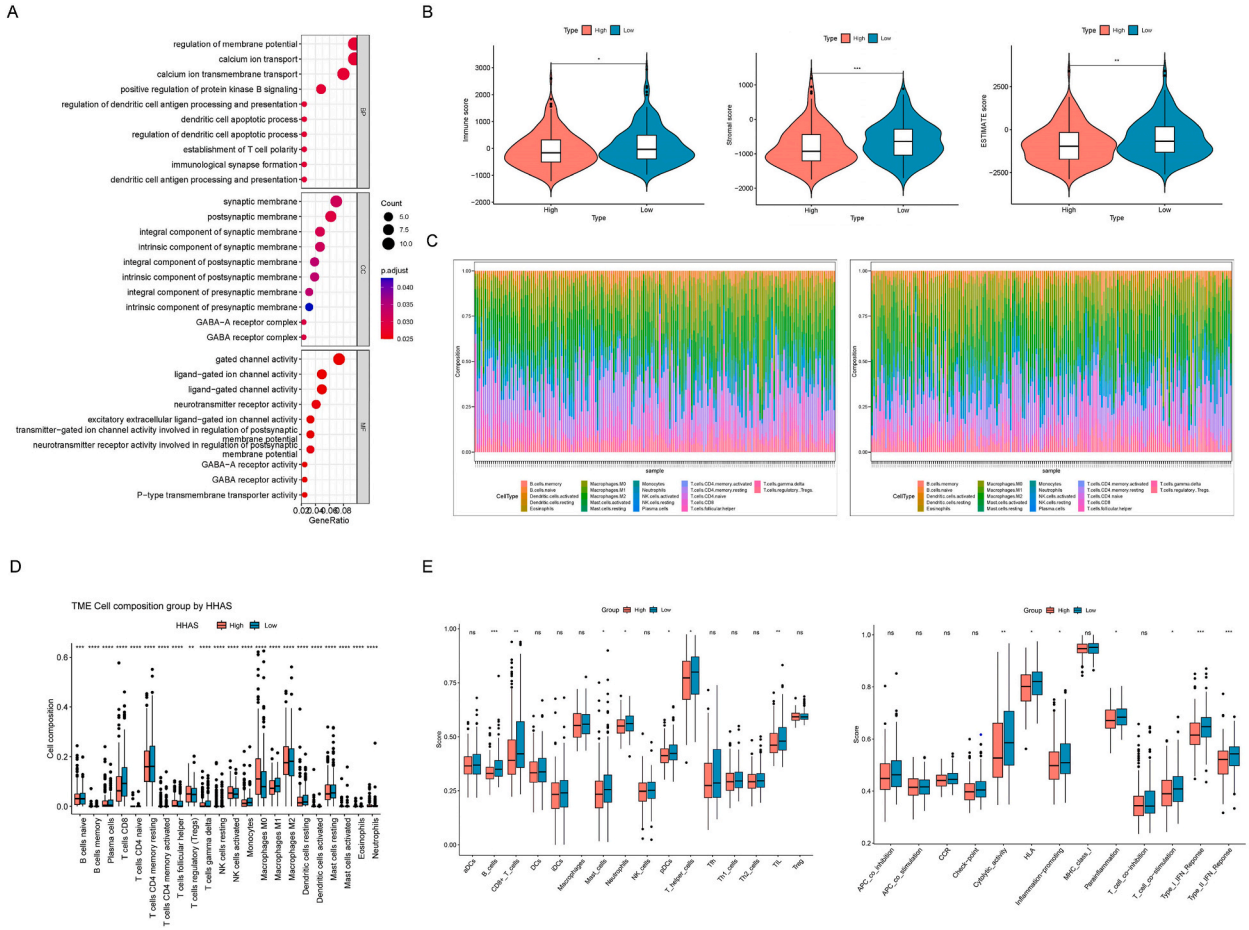

Fig. 8. Immune cell infiltration patterns between high- and low-HHAS groups. (A) GO functional enrichment analysis reveals that differentially expressed genes between high- and low-HHAS groups are associated with innate and adaptive immune system functions. (B) Distribution of immune score, stromal score, and ESTIMATE score is significantly different between high- and low-HHAS groups. (C) Immunocyte profiles of low- and high-HHAS groups based on CIBERSORT algorithm. The left panel shows the immunocyte profile of the low-HHAS group, while the right panel shows that of the high-HHAS group. (D) Significant differences exist in immune cell composition between different HHAS groups. (E) Boxplots showing immune cell and immune-related pathway scores between different HHAS groups based on ssGSEA algorithm. *p < 0.05, **p < 0.01, ***p < 0.001, where the asterisk indicates the level of statistical significance.

undertaken. Employing the CIBERSORT algorithm, an analysis of tumor-infiltrating immune cell (TIC) subtypes was conducted, resulting in a landscape comprising 21 immune cells in the HCC samples (Fig. 8C). Multiple TICs were associated with the HHAS (Fig. 8D). In comparison to the high-HHAS group, the low-HHAS group demonstrated a higher ratio of anti-tumor immune cells, specifically $CD8^+$ T cells and M1 macrophages. This difference underscores the distinct immune profiles between the two HHAS subgroups. Conversely, the high-HHAS group showed a higher proportion of immune-suppressive cells, such as Tregs when compared to the low-HHAS group. This observation implies the existence of an immune-suppressive microenvironment in the high-HHAS group. Utilizing the ssGSEA algorithm, an exploration of the correlation between the HHAS model and immune cells, along with immune-related pathways, was carried out. The outcomes unveiled significantly lower scores for anti-tumor immune cells, including B cells, $CD8^+$ T cells, and tumor-infiltrating lymphocytes, within the high-HHAS group compared to the low-HHAS group (Fig. 8E). This aligns with the results obtained through the CIBERSORT algorithm. Ultimately, diminished scores were observed for immune-related pathways in the high-HHAS group, encompassing the HLA pathway, Inflammation-promoting, T cell co-stimulation, and Type I/II IFN Response. These results further support that the HHAS model can affect the activity of TME in HCC, which may also contribute to the variety clinical outcome.

3.7. *HHAS model forecasts response to immune checkpoint inhibitor (ICI) treatment in HCC*

Given the vital role of the HHAS in shaping the TME, we used the TIDE database to further predict its ability to mediate tumor immune evasion. Our findings indicated a substantial elevation in both TIDE scores and Exclusion scores within the high-HHAS group (Fig. 9A–B), while the Dysfunction score was the opposite (Fig. 9C), indicating a lower response to ICI treatment in the high-HHAS group. Furthermore, the response rate of ICI treatment was assessed in the anti-PD-L1 treatment group (IMvigor210). Notably, individuals exhibiting high HHAS displayed a markedly reduced response rate to Immune Checkpoint Inhibitors (ICI) in comparison to those with low HHAS (Figs. 9D and 27.43% vs 17.81%). This observation emphasizes the potential impact of HHAS on the effectiveness of ICI treatment. The effectiveness of ICI treatment was significantly correlated with the HHAS (Fig. 9E). In addition, it was observed that patients with higher HHAS manifested notably diminished overall survival rates in comparison to those within the low-HHAS group (Fig. 9F). These results underscore the potential of the HHAS model in forecasting immunotherapy response, indicating its valuable role in guiding strategies for ICI treatments.

4. Discussion

The Hedgehog pathway is pivotal in liver development, injury repair, and carcinogenesis [29]. Current studies have exhibited that inhibiting Hedgehog expression can suppress cancer-associated stromal stem cell-driven ovarian tumor immune evasion and

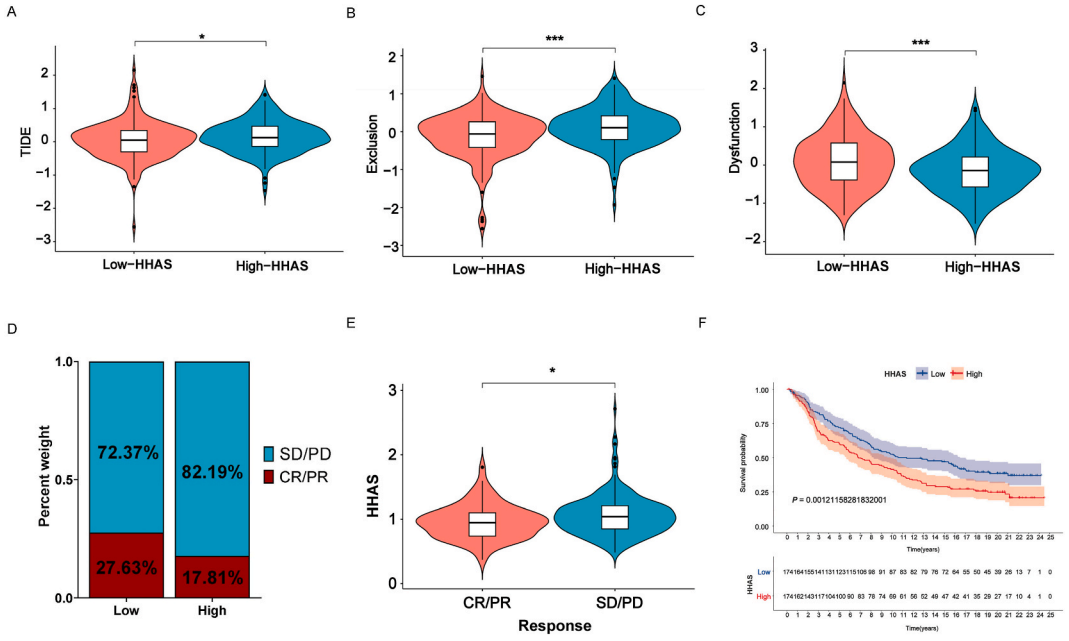

Fig. 9. Immunotherapy response in low- and high-HHAS groups. (A–C) Differences in TIDE, Exclusion, and Dysfunction scores between low- and high-HHAS groups. (D) Proportions of immune checkpoint inhibitor (ICI) response in different HHAS groups from the IMvigor210 dataset. (E) Distribution of HHAS in the CR/PR and SD/PD groups. (F) Kaplan-Meier survival curves demonstrating overall survival differences between high- and low-HHAS groups in the IMvigor210 dataset. CR, complete response; PR, partial response; SD, stable disease; PD, progressive disease. The asterisks denote statistical significance (*$p < 0.05$, **$p < 0.01$, ***$p < 0.001$).

immunotherapy resistance [30], highlighting the Hedgehog signaling pathway as a potential target for cancer immunotherapy. Herein, our study conducted an integrated analysis of the Hedgehog signaling genes' correlation with clinical outcome and immune microenvironment feature. By quantifying the expression of survival-associated Hedgehog genes, we identified three distinct Hedgehog clusters with cluster 3 exhibiting significant associations with poor prognosis and immunosuppressive TME. Furthermore, a tumor prognosis prediction system, HHAS, was formulated to evaluate the Hedgehog pattern of individual HCC cases based on 11 Hedgehog genes. Patients with low HHAS exhibited a higher ratio of $CD8^+$ T cell effector factors and better immunotherapy response, while high HHAS patients demonstrated significant associations with adverse clinical outcomes, high TP53 expression, increased enrichment of immunosuppressive cell.

Our comprehensive study revealed for the first time that alterations of the Hedgehog pathway can serve as important molecular subtypes for HCC. With Hedgehog pathway alterations, 57 Hedgehog-related genes associated with prognosis can stratify patients into three distinct subgroups, including Hedgehog activation (Cluster 3), Hedgehog inactivation (Cluster 2), and moderate Hedgehog activation (Cluster 1). Studies conducted previously have demonstrated that the Hedgehog pathway serves as a key mediator of pancreatic cancer [31] and prostate cancer [32] development. Herein, our study also showed that Hedgehog activation subtype frequently occurs in advanced-stage HCC patients. Additionally, our results also Hedgehog pathway activation exhibit significant increases in Ang-1, Ang-2, CCND1, CCNB1, and FAS expression levels, suggesting that Hedgehog pathway activation may enhance angiogenesis, cell cycle progression, and reduce apoptosis. Therefore, targeting genes associated with Hedgehog signaling may represent a promising therapeutic strategy for advanced-stage HCC treatment. Notably, patients in the subtype of Hedgehog activation have higher TIDE scores, suggesting that Hedgehog activation subtype has a higher immune-suppressive microenvironment. This was validated by immune cell infiltration analysis among subgroups, where immune-suppressive cells, like $CD4^+$ Th2 T cells [33] and immune-suppressive molecule CD274 (PDL1) [34], were mainly enriched in patients with Hedgehog activation subtype. Therefore, for this subset of patients, alternative immunotherapeutic strategies or combination therapy with ICB should be explored to achieve better treatment outcomes.

Secondly, our prognostic scoring model based on hedgehog genes further demonstrated a strong association between hedgehog genes and the TME features. $CD8^+$ T cells are an essential immune cell, with a capability of identification and elimination pathogens and tumor cells [35]. Contrastingly, the pivotal role of regulatory T cells (Tregs) in immune evasion and tumor growth is evident, as they possess the capability to counteract T cell-mediated immune responses [36]. Herein, immune-related pathways exhibited activation in samples with low HHAS. Upon further examination of immune cells, various tumor immune suppressive subgroups were notably elevated in the high HHAS group, including Tregs, whereas anti-tumor immune subgroups like $CD8^+$ T cells were prominently enriched in the low HHAS group. Additionally, higher levels of M0 macrophages were observed in high HHAS samples, while M1 macrophages were enriched in low HHAS samples. Correspondingly, the proportion of TIL cells and dendritic cells also changed, which could be associated with the response of immune cells to the hedgehog pathway in the HCC microenvironment.

Lastly, indications from our study propose that samples with low HHAS might derive greater benefits from ICI treatment. Similar to patients with Hedgehog activation cluster, high HHAS patients are positively correlated with TIDE scores, suggesting their association with immune-suppressive state and a potentially poor response to ICI therapy. Moreover, the high HHAS samples are positively correlated with Exclusion scores and negatively correlated with Dysfunction scores, indicating that immune-suppressive states of these patients mainly stem from immune escape mechanisms in the TME, rather than immunosuppressive cell dysfunction. Further evaluations reveal that high HHAS patients possess a significantly lower response to PD-L1 inhibition and decreased survival quality compared to low HHAS patients. The results of this immunotherapy are consistent with the immune-suppressive state in the TME of patients with high HHAS scores and suggest that the immune-suppressive and immune-escape states of high HHAS samples may be the primary reasons for their poor prognosis. However, further investigations are essential to explore the involvement of HHAS in immune cells, potentially holding substantial clinical implications for optimizing disease treatment and immunotherapy.

Our study comes with certain limitations. Firstly, our data primarily relied on bulk RNA-seq, which offers a lower level of evidence when compared to single-cell sequencing. Therefore, it is imperative to conduct validation using single-cell sequencing in future studies to gain a more comprehensive understanding of cellular-level differences. Secondly, despite our efforts to mitigate batch effects through data standardization, batch effects between different datasets may introduce some degree of bias in our research findings. Lastly, to realize the clinical value of our study results, it is crucial to validate them using large-scale, multi-center clinical cohort data, ensuring credibility and reliability.

Overall, our current study provides a thorough investigation of the immunological activity and therapeutic response of HCC based on Hedgehog-signaling related genes. We reveal that stimulation of the Hedgehog pathway might be intricately linked to decreased TME immunological activity and adverse clinical outcomes in HCC patients. Therefore, developing effective therapies for HCC patients may involve targeting the Hedgehog signaling pathway, presenting a promising strategy.

Funding

This study received grants from the Postdoctoral start-up fund of Guangdong Provincial People's Hospital (BY0120210006), Guangdong Provincial People's Hospital Peak Climbing Plan Project (DFJH201906), National and natural supporting funds of Guangdong Provincial People's Hospital (8197103742), Guangdong Provincial People's Hospital Doctoral Initiation Project (2020bq17), Medical Scientific Technology Research Foundation of Guangdong Province (B2021367).

Institutional review Board Statement

Not applicable

Informed consent Statement

Not applicable.

Data availability Statement

All data utilized in analysis are available.

CRediT authorship contribution statement

Limin Zhen: Writing – original draft, Data curation. **Yi Zhu:** Writing – original draft, Data curation. **Zhen Wu:** Writing – original draft, Data curation. **Jinyao Liao:** Data curation. **Liaoyuan Deng:** Data curation. **Qianqian Ma:** Data curation. **Qili Wu:** Investigation, Conceptualization. **Gang Ning:** Investigation. **Qiuxiong Lin:** Investigation. **Liya Zhou:** Investigation. **Yanjie Huang:** Investigation. **Zewei Zhuo:** Writing – review & editing, Conceptualization. **Ren Chen:** Supervision, Conceptualization. **Dongnan Yu:** Supervision, Conceptualization.

Declaration of competing interest

The authors declare that they have no known competing financial interests or personal relationships that could have appeared to influence the work reported in this paper.

The authors declare that they have no competing interests.

Acknowledgments

We would like to thank TCGA-LICH, ICGC dataset and R software for free use. Fig. 1 created with BioRender.com.

Appendix A. Supplementary data

Supplementary data to this article can be found online at https://doi.org/10.1016/j.heliyon.2024.e26989.

References

[1] R. Lozano, M. Naghavi, K. Foreman, S. Lim, K. Shibuya, V. Aboyans, J. Abraham, T. Adair, R. Aggarwal, S.Y. Ahn, et al., Global and regional mortality from 235 causes of death for 20 age groups in 1990 and 2010: a systematic analysis for the Global Burden of Disease Study 2010, Lancet 380 (9859) (2012) 2095–2128, https://doi.org/10.1016/S0140-6736(12)61728-0.

[2] L. European Association for Study of, R. European Organisation for, C. Treatment of, EASL-EORTC clinical practice guidelines: management of hepatocellular carcinoma, Eur. J. Cancer 48 (5) (2012) 599–641, https://doi.org/10.1016/j.ejca.2011.12.021.

[3] J. Bruix, M. Sherman, American association for the study of liver D: **management of hepatocellular carcinoma: an update**, Hepatology 53 (3) (2011) 1020–1022, https://doi.org/10.1002/hep.24199.

[4] J.M. Llovet, J. Zucman-Rossi, E. Pikarsky, B. Sangro, M. Schwartz, M. Sherman, G. Gores, Hepatocellular carcinoma, Nat Rev Dis Primers 2 (2016) 16018, https://doi.org/10.1038/nrdp.2016.18.

[5] K.J. Wangensteen, K.M. Chang, Multiple roles for hepatitis B and C Viruses and the Host in the development of hepatocellular carcinoma, Hepatology 73 (Suppl 1) (2021) 27–37, https://doi.org/10.1002/hep.31481. Suppl 1.

[6] L. Gong, F. Wei, F.J. Gonzalez, G. Li, Hepatic fibrosis: targeting peroxisome proliferator-activated receptor alpha from mechanism to medicines, Hepatology 78 (5) (2023) 1625–1653, https://doi.org/10.1097/HEP.0000000000000182.

[7] C. Xu, Z. Xu, Y. Zhang, M. Evert, D.F. Calvisi, X. Chen, beta-Catenin signaling in hepatocellular carcinoma, J. Clin. Invest. 132 (4) (2022), https://doi.org/10.1172/JCI154515.

[8] X. Zheng, W. Zeng, X. Gai, Q. Xu, C. Li, Z. Liang, H. Tuo, Q. Liu, Role of the Hedgehog pathway in hepatocellular carcinoma, Oncol. Rep. 30 (5) (2013) 2020–2026, https://doi.org/10.3892/or.2013.2690 (review).

[9] S. Lim, S.M. Lim, M.J. Kim, S.Y. Park, J.H. Kim, Sonic hedgehog pathway as the prognostic marker in patients with extensive stage Small cell lung cancer, Yonsei Med. J. 60 (10) (2019) 898–904, https://doi.org/10.3349/ymj.2019.60.10.898.

[10] Q. Li, Y. Zhang, H. Zhan, Z. Yuan, P. Lu, L. Zhan, W. Xu, The Hedgehog signalling pathway and its prognostic impact in human gliomas, ANZ J. Surg. 81 (6) (2011) 440–445, https://doi.org/10.1111/j.1445-2197.2010.05585.x.

[11] Z. Liu, K. Tu, Y. Wang, B. Yao, Q. Li, L. Wang, C. Dou, Q. Liu, X. Zheng, Hypoxia Accelerates Aggressiveness of hepatocellular carcinoma cells involving Oxidative stress, Epithelial-Mesenchymal Transition and Non-Canonical hedgehog signaling, Cell. Physiol. Biochem. 44 (5) (2017) 1856–1868, https://doi.org/10.1159/000485821.

[12] S. Efroni, D. Meerzaman, C.F. Schaefer, S. Greenblum, M. Soo-Lyu, Y. Hu, C. Cultraro, E. Meshorer, K.H. Buetow, Systems analysis utilising pathway interactions identifies sonic hedgehog pathway as a primary biomarker and oncogenic target in hepatocellular carcinoma, IET Syst. Biol. 7 (6) (2013) 243–251, https://doi.org/10.1049/iet-syb.2010.0078.

[13] Cancer Genome Atlas Research Network, Electronic address wbe, cancer Genome Atlas research N: **comprehensive and integrative genomic Characterization of hepatocellular carcinoma**, Cell 169 (7) (2017) 1327–1341 e1323, https://doi.org/10.1016/j.cell.2017.05.046.

[14] C.C. Hui, S. Angers, Gli proteins in development and disease, Annu. Rev. Cell Dev. Biol. 27 (2011) 513–537, https://doi.org/10.1146/annurev-cellbio-092910-154048.
[15] P.A. Beachy, S.S. Karhadkar, D.M. Berman, Tissue repair and stem cell renewal in carcinogenesis, Nature 432 (7015) (2004) 324–331, https://doi.org/10.1038/nature03100.
[16] J. Jiang, C.C. Hui, Hedgehog signaling in development and cancer, Dev. Cell 15 (6) (2008) 801–812, https://doi.org/10.1016/j.devcel.2008.11.010.
[17] J. Briscoe, P.P. Therond, The mechanisms of Hedgehog signalling and its roles in development and disease, Nat. Rev. Mol. Cell Biol. 14 (7) (2013) 416–429, https://doi.org/10.1038/nrm3598.
[18] A. de Reynies, D. Javelaud, N. Elarouci, V. Marsaud, C. Gilbert, A. Mauviel, Large-scale pan-cancer analysis reveals broad prognostic association between TGF-beta ligands, not Hedgehog, and GLI1/2 expression in tumors, Sci. Rep. 10 (1) (2020) 14491, https://doi.org/10.1038/s41598-020-71559-w.
[19] A. Ballester, A. Guijarro, B. Bravo, J. Hernandez, R. Murillas, M.I. Gallego, S. Ballester, Hedgehog signalling Modulates immune response and Protects against Experimental Autoimmune Encephalomyelitis, Int. J. Mol. Sci. 23 (6) (2022), https://doi.org/10.3390/ijms23063171.
[20] J.T. Leek, W.E. Johnson, H.S. Parker, A.E. Jaffe, J.D. Storey, The sva package for removing batch effects and other unwanted variation in high-throughput experiments, Bioinformatics 28 (6) (2012) 882–883, https://doi.org/10.1093/bioinformatics/bts034.
[21] M.E. Ritchie, B. Phipson, D. Wu, Y. Hu, C.W. Law, W. Shi, G.K. Smyth, Limma powers differential expression analyses for RNA-sequencing and microarray studies, Nucleic Acids Res. 43 (7) (2015) e47, https://doi.org/10.1093/nar/gkv007.
[22] M.D. Wilkerson, D.N. Hayes, ConsensusClusterPlus: a class discovery tool with confidence assessments and item tracking, Bioinformatics 26 (12) (2010) 1572–1573, https://doi.org/10.1093/bioinformatics/btq170.
[23] G. Sturm, F. Finotello, F. Petitprez, J.D. Zhang, J. Baumbach, W.H. Fridman, M. List, T. Aneichyk, Comprehensive evaluation of transcriptome-based cell-type quantification methods for immuno-oncology, Bioinformatics 35 (14) (2019) i436–i445, https://doi.org/10.1093/bioinformatics/btz363.
[24] P. Blanche, J.F. Dartigues, H. Jacqmin-Gadda, Estimating and comparing time-dependent areas under receiver operating characteristic curves for censored event times with competing risks, Stat. Med. 32 (30) (2013) 5381–5397, https://doi.org/10.1002/sim.5958.
[25] A. Mayakonda, D.C. Lin, Y. Assenov, C. Plass, H.P. Koeffler, Maftools: efficient and comprehensive analysis of somatic variants in cancer, Genome Res. 28 (11) (2018) 1747–1756, https://doi.org/10.1101/gr.239244.118.
[26] S. Hanzelmann, R. Castelo, J. Guinney, GSVA: gene set variation analysis for microarray and RNA-seq data, BMC Bioinf. 14 (2013) 7, https://doi.org/10.1186/1471-2105-14-7.
[27] M. Kim, H. Mun, C.O. Sung, E.J. Cho, H.J. Jeon, S.M. Chun, D.J. Jung, T.H. Shin, G.S. Jeong, D.K. Kim, et al., Patient-derived lung cancer organoids as in vitro cancer models for therapeutic screening, Nat. Commun. 10 (1) (2019) 3991, https://doi.org/10.1038/s41467-019-11867-6.
[28] P. Jiang, S. Gu, D. Pan, J. Fu, A. Sahu, X. Hu, Z. Li, N. Traugh, X. Bu, B. Li, et al., Signatures of T cell dysfunction and exclusion predict cancer immunotherapy response, Nat Med 24 (10) (2018) 1550–1558, https://doi.org/10.1038/s41591-018-0136-1.
[29] H. Kwon, K. Song, C. Han, W. Chen, Y. Wang, S. Dash, K. Lim, T. Wu, Inhibition of hedgehog signaling ameliorates hepatic inflammation in mice with nonalcoholic fatty liver disease, Hepatology 63 (4) (2016) 1155–1169, https://doi.org/10.1002/hep.28289.
[30] S. Cascio, C. Chandler, L. Zhang, S. Sinno, B. Gao, S. Onkar, T.C. Bruno, D.A.A. Vignali, H. Mahdi, H.U. Osmanbeyoglu, et al., Cancer-associated MSC drive tumor immune exclusion and resistance to immunotherapy, which can be overcome by Hedgehog inhibition, Sci. Adv. 7 (46) (2021) eabi5790, https://doi.org/10.1126/sciadv.abi5790.
[31] A. Neesse, C.A. Bauer, D. Ohlund, M. Lauth, M. Buchholz, P. Michl, D.A. Tuveson, T.M. Gress, Stromal biology and therapy in pancreatic cancer: ready for clinical translation? Gut 68 (1) (2019) 159–171, https://doi.org/10.1136/gutjnl-2018-316451.
[32] G. Shaw, A.M. Price, E. Ktori, I. Bisson, P.E. Purkis, S. McFaul, R.T. Oliver, D.M. Prowse, Hedgehog signalling in androgen independent prostate cancer, Eur. Urol. 54 (6) (2008) 1333–1343, https://doi.org/10.1016/j.eururo.2008.01.070.
[33] P. Storz, H.C. Crawford, Carcinogenesis of pancreatic Ductal Adenocarcinoma, Gastroenterology 158 (8) (2020) 2072–2081, https://doi.org/10.1053/j.gastro.2020.02.059.
[34] K. Shimada, F. Hayakawa, H. Kiyoi, Biology and management of primary effusion lymphoma, Blood 132 (18) (2018) 1879–1888, https://doi.org/10.1182/blood-2018-03-791426.
[35] E.J. Wherry, T cell exhaustion, Nat. Immunol. 12 (6) (2011) 492–499, https://doi.org/10.1038/ni.2035.
[36] S.H. Baumeister, G.J. Freeman, G. Dranoff, A.H. Sharpe, Coinhibitory pathways in immunotherapy for cancer, Annu. Rev. Immunol. 34 (2016) 539–573, https://doi.org/10.1146/annurev-immunol-032414-112049.